Journal of Chemical&Engineering Data

pubs.acs.org/jced Article

Monoethanolamine + Ethylene Glycol + Choline Chloride: An Effect of the Mixture Composition on the CO_2 Absorption Capacity, Density, and Viscosity

Olga V. Kazarina,* Vira N. Agieienko, Anton N. Petukhov, Andrey V. Vorotyntsev, Alexander S. Kazarin, Maria E. Atlaskina, Artem A. Atlaskin, Artyom N. Markov, Anna A. Golovacheva, and Ilya V. Vorotyntsev

Cite This: *J. Chem. Eng. Data* 2022, 67, 2899–2912 Read Online

ACCESS | Metrics & More | Article Recommendations | Supporting Information

Downloaded via UNIV SCIENCE AND TECHNOLOGY CHINA on October 29, 2024 at 09:26:56 (UTC).
See https://pubs.acs.org/sharingguidelines for options on how to legitimately share published articles.

ABSTRACT: In the present paper, a systematic investigation of the influence of amine and salt concentration on the CO_2 absorption capacity (m_{CO_2}, moles of CO_2 absorbed by 1 kg of a solution) and amine efficiency (c_{CO_2}, moles of CO_2 absorbed by 1 mole of amine) of the ternary mixtures composed of monoethanolamine (MEA), ethylene glycol (EG), and choline chloride (ChCl) was carried out. We demonstrate that, in general, the presence of a fixed amount of ChCl in a mixed {MEA + EG} solvent cannot improve m_{CO_2} over an entire range of solvent composition and weakly decreases c_{CO_2} with the effect more pronounced for the mixtures containing greater amount of MEA. The influence of ChCl concentration on the above properties was analyzed for the mixtures with a fixed MEA/EG mole ratio but various ChCl concentrations. It was shown that a decrease in m_{CO_2} observed with an increase in ChCl, again, is rather caused by an overall decrease in MEA content in a mixture as its efficiency c_{CO_2} does not change when ChCl concentration increases. In addition, properties such as density (ρ) and viscosity (η) of the binary {MEA + EG} and ternary {MEA + EG + ChCl} mixtures were obtained within a wide range of temperatures for both neat and CO_2-loaded samples. We show that regardless of the {MEA + EG} mixed solvent composition, the presence of ChCl increases both ρ and η. For CO_2-loaded samples, both properties increase significantly with a greater contribution for the mixtures containing greater amount of MEA.

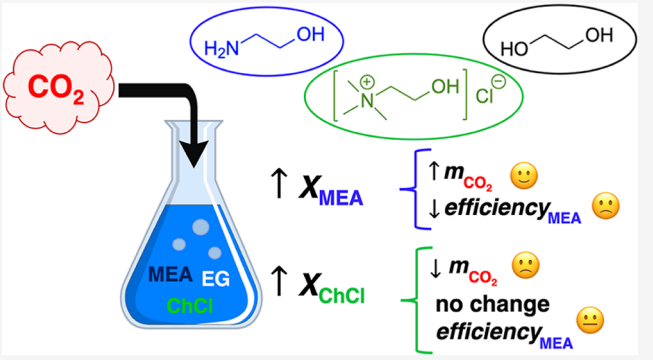

INTRODUCTION

Despite significant progress in development and a global rollout of the renewable energy sources, natural gas and other fossil fuels sustain the leading position in the power source market. Due to the well-developed infrastructure and relatively low mining cost, they are highly expected to dominate the market in the near future.[1] As a consequence, it is anticipated that the annual anthropogenic emission of greenhouse gases including carbon dioxide into the atmosphere will constantly increase, provoking thus the global warming and climate changing processes. In this regard, removing CO_2 from the exhaust streams is of particular importance for environmental and atmosphere protection.

In the past decades, the carbon capture, utilization, and storage (CCUS) technologies aimed at reducing the negative impact of CO_2 have been intensively developed. The main principle of CCUS is to reduce the redundant CO_2 for subsurface storage in depleted reservoirs such as hydrocarbon reservoirs,[2] coal seams[3] and chalk formations,[4] in saline aquifers,[5,6] by sequestration *via* gas hydrates,[7−9] by conversion into the valued products obtained by the methanation reaction[10] or by a reaction with olefin oxides,[11] by utilization with supercritical CO_2 Brayton cycles,[12] and many others.[8,13,14] An economical attractiveness of these industrial life cycles lies in the possibility of a pipeline transfer of CO_2 from a combustion chamber to the sequestration sites, which allows utilizing huge amounts of the produced gas.[15]

Nevertheless, a conventional technology of wet absorption by amines and their aqueous solutions is still widely used for capturing CO_2. Its undeniable advantages include a wide degree of industrialization,[16,17] recyclability of absorbents, and lower harm in comparison with, for example, absorption by alkali solutions,[18] a possibility of temporary CO_2 fixing with

Received: April 15, 2022
Accepted: August 11, 2022
Published: September 2, 2022

© 2022 American Chemical Society

https://doi.org/10.1021/acs.jced.2c00245
J. Chem. Eng. Data 2022, 67, 2899−2912

Table 1. Chemicals used in This Work

chemical	CAS no	abbr	source	mass % purity[a]	purification	initial water content (ppm)[b]	drying
choline chloride	67-48-1	ChCl	Acros Organics	99	used without further purification	6000	
ethylene glycol	107-21-1	EG	KomponentReaktiv (Russia)	>99.6	used without further purification	700	activated 3 Å molecular sieves
monoethanolamine	141-43-5	MEA	"Oka-Sintez" Ltd (Russia)	>97	vacuum distillation	2000	activated 3 Å molecular sieves
NH_4SCN	1762-95-4		KomponentReaktiv (Russia)	99	recrystallization	260	drying under reduced pressure
glycerol	56-81-5	Gly	KomponentReaktiv (Russia)	>99.6	used without further purification	600	activated 3 Å molecular sieves
nitrogen	7727-37-9	N_2	Monitoring (Russia)	99.9999	used without further purification		
carbon dioxide	124-38-9	CO_2	Monitoring (Russia)	99.9999	used without further purification		
ammonia	7664-41-7	NH_3	Ltd "Horst"	99.99999	used without purification		
water	7732-18-5	H_2O	Millipore Milli-Q				

[a]Provided by a supplier. [b]Mass fraction ($w_{H_2O} = m_{H_2O}/m_{sample}$).

Table 2. Densities (ρ) of the Mixtures of MEA (1) and EG (2) at Temperatures (T) and EG Mole Fraction (x_2) at P = 0.1 MPa[a]

	ρ (g·cm^{-3})								
T(K)	x_2 = 0.000	0.126	0.250	0.364	0.517	0.629	0.747	0.873	1.000
278.15									1.125
283.15									1.121
288.15	1.020	1.035	1.050	1.061	1.077	1.086	1.098	1.109	1.117
293.15	1.016	1.031	1.045	1.057	1.073	1.083	1.094	1.105	1.114
298.15	1.012	1.027	1.041	1.053	1.069	1.079	1.090	1.101	1.110
303.15	1.008	1.023	1.038	1.049	1.065	1.076	1.087	1.098	1.107
308.15	1.004	1.019	1.034	1.045	1.062	1.071	1.083	1.094	1.103
313.15	1.000	1.015	1.030	1.042	1.058	1.068	1.079	1.091	1.100
318.15	0.996	1.011	1.026	1.038	1.054	1.064	1.076	1.087	1.096
323.15	0.992	1.007	1.022	1.034	1.051	1.060	1.072	1.083	1.093
328.15	0.988	1.003	1.018	1.030	1.047	1.057	1.068	1.080	1.089
333.15	0.984	1.000	1.014	1.026	1.043	1.053	1.065	1.076	1.085
338.15	0.980	0.996	1.011	1.023	1.039	1.049	1.061	1.073	1.082
343.15	0.976	0.992	1.007	1.019	1.036	1.046	1.058	1.069	1.078
348.15	0.972	0.988	1.003	1.015	1.032	1.042	1.054	1.065	1.075
353.15	0.968	0.984	0.999	1.011	1.028	1.038	1.050	1.061	1.071
358.15	0.964	0.980	0.995	1.007	1.024	1.034	1.046	1.058	1.067
363.15	0.960	0.976	0.991	1.003	1.020	1.030	1.042	1.054	1.063

[a]Standard uncertainties are $u(x_i)$ = 0.001, $u(T)$ = 0.01 K, and $u(P)$ = 10 kPa. The relative expanded uncertainty is $U_r(\rho)$ = 0.001 (0.95 level of confidence).

further accumulation,[19] and customization for favorable industrial processes due to diversity in the compound structure.[20] The most commonly used amines are alkanolamines such as monoethanolamine (MEA) and 2-amino-2-methyl-1-propanol (AMP), diethanolamine (DEA) and diisopropanolamine (DIPA), and *N*-methyl-diethanolamine (MDEA) and triethanolamine (TEA), being pairwise primary, secondary, and tertiary amines, respectively.[19,21,22] However, the sufficient drawback of the abovementioned type of absorption is water and anime evaporation, the factors mainly responsible for the high energy consumption and equipment corrosion.[23]

In view of these considerations, using high-boiling solvents instead of water can be an option due to a synergy between lower solvent heat capacity and reduced solvent vaporization loss.[24] Also, it was shown that the lower dielectric constant of nonaqueous solvents compared to that of water reduces stability of the formed CO_2-retaining products bicarbonate and carbamate and thus facilitates the desorption process.[25,26] Recent publications on the high-boiling point solvents with regard to CO_2 capture include papers focusing on investigation of the amine solutions in glycols[23,27−32] and their mixtures with primary alcohols,[27,31,33] in glycol ethers,[34] propylene carbonate,[28] *N*-methyl formamide,[27] *N*-methyl pyrrolidone (NMP), and many others. In their research paper, Barzagli and co-workers[33] came to the conclusion that lower heat capacity and evaporation enthalpy of the studied organic solvents and lower stripping temperature in comparison to those of water and aqueous alkanolamines, respectively, should reduce the amine evaporation and degradation and equipment corrosion. In a later work,[35] the authors showed that although aqueous solutions exhibit high CO_2 absorption capacity due to the formation of bicarbonate in non-aqueous solutions, the absorption rates are increased, thanks to formation of the

https://doi.org/10.1021/acs.jced.2c00245
J. Chem. Eng. Data 2022, 67, 2899−2912

Table 3. Densities (ρ) of the Mixtures of MEA (1), EG (2), and ChCl (3) at Temperatures (T), Constant ChCl Mole Fraction of x_3 = 0.111, and Various EG Mole Fractions (x_2) at P = 0.1 MPa[a]

	ρ (g·cm^{-3})								
T (K)	x_2 = 0.000	0.111	0.222	0.324	0.453	0.558	0.664	0.776	0.889
293.15	1.045	1.056	1.066	1.074	1.085	1.093	1.101	1.110	1.117
298.15	1.041	1.052	1.062	1.071	1.081	1.090	1.098	1.107	1.114
303.15	1.038	1.049	1.059	1.068	1.078	1.087	1.095	1.103	1.111
308.15	1.034	1.045	1.055	1.064	1.075	1.083	1.092	1.100	1.108
313.15	1.031	1.042	1.052	1.061	1.071	1.080	1.088	1.097	1.105
318.15	1.027	1.038	1.048	1.057	1.068	1.077	1.085	1.094	1.101
323.15	1.023	1.035	1.045	1.054	1.065	1.073	1.082	1.091	1.098
328.15	1.020	1.031	1.041	1.050	1.061	1.070	1.079	1.088	1.095
333.15	1.016	1.028	1.038	1.047	1.058	1.067	1.075	1.084	1.092
338.15	1.012	1.024	1.034	1.044	1.055	1.064	1.072	1.081	1.089
343.15	1.009	1.020	1.031	1.040	1.051	1.060	1.067	1.077	1.086
348.15	1.005	1.017	1.027	1.037	1.048	1.057	1.066	1.074	1.082
353.15	1.002	1.013	1.024	1.033	1.045	1.054	1.062	1.071	1.079
358.15	0.998	1.010	1.020	1.030	1.041	1.050	1.059	1.068	1.076
363.15	0.994	1.006	1.017	1.026	1.038	1.047	1.056	1.064	1.073

[a]Standard uncertainties are $u(x_i)$ = 0.001, $u(T)$ = 0.01 K, and $u(P)$ = 10 kPa. The relative expanded uncertainty is $U_r(\rho)$ = 0.001 (0.95 level of confidence).

Table 4. Densities (ρ) of the Mixtures of MEA (1), EG (2), and ChCl (3) at Temperatures (T), a Constant MEA to EG Ratio of x_1/x_2= 0.339, and Various ChCl Mole Fractions (x_3) at P = 0.1 MPa[a]

	ρ (g·cm^{-3})									
T (K)	x_3 = 0.000	0.005	0.010	0.025	0.050	0.075	0.100	0.135	0.170	0.215
288.15	1.097	1.097	1.099	1.099	1.101	1.103	1.104	1.106	1.108	1.110
293.15	1.093	1.094	1.094	1.096	1.098	1.099	1.101	1.103	1.105	1.107
298.15	1.089	1.090	1.091	1.092	1.095	1.096	1.098	1.100	1.102	1.104
303.15	1.086	1.086	1.087	1.089	1.091	1.093	1.095	1.097	1.099	1.101
308.15	1.082	1.083	1.084	1.085	1.088	1.089	1.092	1.093	1.096	1.098
313.15	1.079	1.079	1.080	1.082	1.084	1.086	1.088	1.090	1.093	1.096
318.15	1.075	1.076	1.077	1.078	1.081	1.083	1.085	1.087	1.090	1.092
323.15	1.071	1.072	1.073	1.075	1.077	1.079	1.082	1.084	1.086	1.089
328.15	1.068	1.069	1.069	1.071	1.074	1.076	1.078	1.081	1.083	1.085
333.15	1.064	1.065	1.066	1.068	1.070	1.073	1.075	1.077	1.080	1.082
338.15	1.060	1.061	1.062	1.064	1.067	1.069	1.072	1.074	1.077	1.079
343.15	1.057	1.058	1.058	1.061	1.064	1.066	1.068	1.071	1.074	1.076
348.15	1.053	1.054	1.055	1.057	1.060	1.062	1.065	1.068	1.071	1.073
353.15	1.049	1.050	1.051	1.053	1.057	1.059	1.062	1.065	1.068	1.070
358.15	1.045	1.046	1.047	1.050	1.053	1.056	1.058	1.061	1.065	1.067
363.15	1.041	1.042	1.044	1.046	1.049	1.052	1.055	1.058	1.061	1.064

[a]Standard uncertainties are $u(x_i)$ = 0.001, $u(T)$ = 0.01 K, and $u(P)$ = 10 kPa. The relative expanded uncertainty is $U_r(\rho)$ = 0.001 (0.95 level of confidence).

kinetically favored amine carbamates. Bihong *et al.*[32] and Barbarossa *et al.*[31] found that carbamates also form with amines in NMP solution and EG/ethanol mixtures, respectively. In both groups, the authors obtained lower solvent loss during the course of the CO_2 desorption step which, in combination with their non-corrosive behavior, makes the studied solutions promising candidates for the CO_2 capture. By combining amine CO_2 absorption in organic solvents and microwave regeneration technique, Bougie *et al.*[27] achieved 78% reduced energy consumption in comparison to that of the traditional 30% MEA aqueous solution.

The above findings reveal that high-boiling point solvents and related mixtures have a great potential in improving CO_2 capture technology. In terms of current interests and novel calls, deep eutectic solvents (DESs) seem to be good candidates for replacing water as CO_2-absorbing solutions. DESs themselves have been widely studied as carbon dioxide absorbents as discussed in detail in a series of the review papers,[36−38] but if not specified by a superbase,[39−42] their absorption capacities are still lower than those for amines and their solutions. Nevertheless, the systems comprising DESs and amines are of particular interest when optimization of the CO_2 absorption technology is considered. Despite significant progress in this area, there have been only a few publications providing systematic investigation of the effect of the system composition, amine structure, and its concentration on the CO_2 capture of the {amine + DES} systems.[43−45] In this work, we show that how the ratio of amine to molecular solvent and electrolyte concentration affect density, viscosity, and CO_2 absorption capacity of the systems composed of choline chloride (ChCl), EG, and MEA within a wide temperature range.

https://doi.org/10.1021/acs.jced.2c00245
J. Chem. Eng. Data 2022, 67, 2899−2912

Table 5. Viscosities (η) of the Mixtures of MEA (1) and EG (2) at Temperatures (T) and EG Mole Fraction (x_2) at P = 0.1 MPa[a]

	η (mPa·s)								
T(K)	x_2 = 0.000	0.126	0.250	0.364	0.517	0.629	0.747	0.873	1.000
278.15									43.5
283.15									33.7
288.15	31.0	39.7	45.3	47.9	45.6	42.4	37.1	31.4	26.6
293.15	23.9	30.2	34.7	36.5	35.2	32.8	29.2	25.0	21.1
298.15	18.7	23.4	27.0	28.5	27.7	25.9	23.2	20.0	17.0
303.15	14.9	18.6	21.3	22.6	22.1	20.8	18.8	16.3	13.9
308.15	12.0	14.8	17.0	18.0	17.8	16.8	15.3	13.4	11.5
313.15	9.79	12.0	13.7	14.6	14.5	13.7	12.6	11.1	9.58
318.15	8.14	9.87	11.3	12.0	12.0	11.4	10.5	9.31	8.12
323.15	6.78	8.15	9.28	9.86	9.91	9.47	8.81	7.84	6.88
328.15	5.77	6.89	7.82	8.31	8.38	8.05	7.52	6.74	5.95
333.15	4.90	5.80	6.57	6.98	7.06	6.81	6.40	5.77	5.12
338.15	4.25	5.00	5.64	5.99	6.09	5.89	5.56	5.04	4.50
343.15	3.69	4.32	4.85	5.16	5.25	5.10	4.82	4.41	3.95
348.15	3.22	3.75	4.20	4.47	4.56	4.44	4.22	3.88	3.49
353.15	2.82	3.27	3.65	3.87	3.96	3.87	3.69	3.41	3.08
358.15	2.51	2.89	3.22	3.42	3.51	3.44	3.29	3.05	2.78
363.15	2.24	2.56	2.85	3.02	3.10	3.05	2.93	2.73	2.49

[a]Standard uncertainties are $u(x_i)$ = 0.001, $u(T)$ = 0.01 K, and $u(P)$ = 10 kPa. The relative expanded uncertainty for viscosity is $U_r(\eta)$ = 0.02 (0.95 level of confidence).

Table 6. Viscosities (η) of the Mixtures of MEA (1), EG (2), and ChCl (3) at Temperatures (T), a Constant ChCl Mole Fraction of x_3 = 0.111, and Various EG Mole Fractions (x_2) at P = 0.1 MPa[a]

	η (mPa·s)								
T(K)	x_2 = 0.000	0.112	0.222	0.324	0.453	0.558	0.664	0.776	0.889
293.15	46.3	52.6	55.2	55.0	49.8	43.7	37.0	30.9	24.7
298.15	35.4	40.2	42.3	42.5	38.9	34.6	29.7	25.2	20.3
303.15	27.6	31.3	33.1	33.4	30.9	27.8	24.1	20.8	16.8
308.15	21.8	24.6	26.1	26.4	24.8	22.5	19.8	17.3	14.1
313.15	17.5	19.7	20.9	21.2	20.1	18.4	16.4	14.4	11.8
318.15	14.2	16.0	17.0	17.3	16.6	15.3	13.7	12.2	10.1
323.15	11.7	13.1	14.0	14.3	13.8	12.8	11.6	10.4	8.64
328.15	9.80	10.9	11.6	11.9	11.6	10.8	9.89	8.97	7.54
333.15	8.30	9.23	9.81	10.1	9.85	9.29	8.53	7.73	6.54
338.15	7.07	7.83	8.32	8.58	8.41	7.99	7.38	6.79	5.80
343.15	6.09	6.72	7.14	7.37	7.27	6.94	6.46	5.97	5.13
348.15	5.28	5.82	6.18	6.39	6.33	6.08	5.69	5.29	4.57
353.15	4.60	5.05	5.40	5.59	5.57	5.38	5.01	4.67	4.07
358.15	4.08	4.47	4.74	4.91	4.91	4.77	4.50	4.21	3.70
363.15	3.62	3.96	4.19	4.35	4.37	4.27	4.04	3.79	3.35

[a]Standard uncertainties are $u(x_i)$ = 0.001, $u(T)$ = 0.01 K, and $u(P)$ = 10 kPa. The relative expanded uncertainty for viscosity is $U_r(\eta)$ = 0.02 (0.95 level of confidence).

EXPERIMENTAL SECTION

Materials. ChCl (99 wt %) was purchased from Acros Organics, and EG (>99 wt %), NH_4SCN (99%), and glycerol (>99 wt %) were purchased from KomponentReaktiv, Russia. MEA (>97) was provided by "Oka-Sintez" Ltd (Russia), Russia, and distilled under vacuum. Prior to use, solvents were stored over freshly activated 3 Å molecular sieves in a desiccator filled with phosphorus pentoxide. Carbon dioxide (99.999 wt %) and nitrogen (99.999 wt %) were purchased from Monitoring, Russia; ammonia (99.9999 wt %) was supplied by Ltd "Horst", Russia. An overview of the substances used in the present work is given in Table 1.

Mixture Preparation. Depending on a series of measurements, {MEA + EG} mixtures covering the entire miscibility range and {MEA + EG + ChCl} mixtures of the concentrations highlighted in Tables 2−7 were prepared by weighing appropriate amounts of neat solvents and/or their mixtures and ChCl stock solutions in EG or the {MEA + EG} mixture on an analytical balance (measuring to 0.1 mg) into tightly sealed vials. After fully mixing the mixture components, the samples were stored over the freshly activated 3 Å molecular sieves in a desiccator filled with P_2O_5. The individual component concentrations in the mixture were expressed in terms of their mole fractions

https://doi.org/10.1021/acs.jced.2c00245
J. Chem. Eng. Data 2022, 67, 2899−2912

Table 7. Viscosities (η) of the Mixtures of MEA (1), EG (2), and ChCl (3) at Temperatures (T), a Constant MEA to EG Ratio of x_1/x_2 = 0.339, and Various ChCl Mole Fractions (x_3) at P = 0.1 MPa[a]

	η (mPa·s)									
T (K)	x_3 = 0.000	0.005	0.010	0.025	0.050	0.075	0.100	0.135	0.170	0.215
288.15	37.4	37.8	37.7	38.7	40.1	42.5	45.0	49.4	55.1	65.5
293.15	29.3	29.6	29.7	30.4	31.6	33.2	35.2	38.6	43.2	51.2
298.15	23.3	23.6	23.7	24.3	25.3	26.6	28.2	30.9	34.5	40.8
303.15	18.8	19.1	19.2	19.7	20.5	21.6	22.9	25.1	28.0	33.0
308.15	15.4	15.5	15.6	16.1	16.8	17.7	18.8	20.5	22.9	26.9
313.15	12.6	12.8	12.8	13.2	13.8	14.5	15.5	17.0	19.0	22.2
318.15	10.5	10.7	10.7	11.1	11.6	12.2	13.0	14.2	15.9	18.6
323.15	8.81	8.93	8.99	9.28	9.75	10.3	11.0	12.0	13.4	15.6
328.15	7.52	7.63	7.68	7.94	8.35	8.81	9.37	10.3	11.5	13.3
333.15	6.40	6.49	6.53	6.77	7.13	7.52	8.01	8.86	9.87	11.4
338.15	5.55	5.64	5.68	5.89	6.21	6.56	6.99	7.66	8.54	9.87
343.15	4.82	4.91	4.94	5.12	5.42	5.72	6.10	6.70	7.46	8.61
348.15	4.22	4.29	4.32	4.49	4.76	5.03	5.36	5.89	6.57	7.56
353.15	3.69	3.76	3.78	3.94	4.17	4.41	4.72	5.18	5.83	6.70
358.15	3.29	3.35	3.37	3.51	3.73	3.95	4.23	4.65	5.18	5.95
363.15	2.93	2.98	3.01	3.13	3.34	3.53	3.78	4.16	4.64	5.32

[a]Standard uncertainties are $u(x_i)$ = 0.001, $u(T)$ = 0.01 K, and $u(P)$ = 10 kPa. The relative expanded uncertainty for viscosity is $U_r(\eta)$ = 0.02 (0.95 level of confidence).

$$x_i = \frac{m_i/M_i}{\sum m_i/M_i} \quad (1)$$

where m_i represents the used masses and M_1 = 61.08, M_2 = 62.07, and M_3 = 139.62 g·mol^{-1} are the molar masses of MEA, EG, and ChCl, respectively.

All operations associated with sample preparation were carried out in a stream of dry nitrogen to avoid contact of the samples with air during the measurement procedures for ρ, η, and CO_2 absorption capacity. Syringe techniques were used to transfer the samples to the N_2-purged measurement cells.

Prior to measurements, a mass water content, $w_{H_2O} = m_{H_2O}/m_{sample}$, expressed in parts per million (ppm) was determined by means of coulometric Karl Fischer titration (Metrohm 831 AG). The data on w_{H_2O} for all of the studied samples are collected in Table S1.

Viscosity and Density Measurements. The density and dynamic viscosity were obtained at atmospheric pressure using a Stabinger SVM3001 viscometer (Anton Paar, Austria) characterized by density and viscosity repeatability of 0.00005 g·cm^{-3} and 0.1%, respectively, and a temperature stability of 0.005 K. The instrument was calibrated by using APS3, APN7.5, APN26, and APN415 calibration oils (Anton Paar, Austria) at T = 293.15, 333.15, and 373.15 K. With the uncertainties arising from the measurement protocol, the nominal uncertainties in density measurements were found to be $u(\rho)$ = 0.05 g·cm^{-3}. Although the corresponding data summarized in Tables 2−4 are given to this number of digits due to the limited purity of the samples,[46] the relative expanded standard uncertainty is equal to $U_r(\rho) \approx 0.001$ (0.95 level of confidence). For viscosity, the estimated relative expanded uncertainty was found to be $U_r(\eta)$ = 0.02 (0.95 level of confidence).

The properties were determined in steps of 5 K within the temperature range of T = (278.15 to 363.15) K for neat EG, T = (288.15 to 363.15) K for neat MEA, and T = (293.15 to 363.15) K for {EA + EG} and {ChCl + MEA + EG} mixtures. For the CO_2-saturated samples, the measurements were performed at ambient pressure and temperatures from T = (288.15 to 318.15) K. However, due to a partial gas release and/or extremely high viscosity of some samples, the measurements were impossible to be carried out at T > 308.15 K or T < 293.15 K, respectively (see the corresponding tables for details). In any case, here we note that the corresponding density and viscosity data are rather given to provide a general trend of a property change while capturing CO_2 using the studied systems.

Verification of the density and viscosity measurements was carried out with oil standards N7.5, N26, and N415. The data are displayed in Figure S1 as deviations (δ) of the experimentally obtained data (Y^{exp}) from the fit (Y^{fit})

$$\delta = \frac{Y^{exp} - Y^{fit}}{Y^{fit}} \quad (2)$$

performed by using the data provided by the supplier for the delivered oil batches with eqs 3 and 7 for density and viscosity, respectively. As seen, the deviations never exceeded the $-0.075 \le 100\delta \le +0.08$ interval for density (a−c) and $-1.9 \le 100\delta \le +1.2$ for viscosity (d−f), that is, they are below the estimated expanded uncertainties, $U_r(\rho)$ = 0.001 and $U_r(\eta)$ = 0.02, respectively.

CO_2 Absorption Capacity. The CO_2 absorption behavior was studied by a weighting method as follows. An accurate mass of the sample (about 10.0 g) was added into a glass tube with an inner diameter of 12 mm and a length of 200 mm. Gas was bubbled through the sample at a flow rate of 20 cm^3•min^{-1} at P = 0.1 MPa, controlled using an electronic pressure sensor with an accuracy of 100 Pa. During the course of measurements, the reaction mixture was constantly mixed using a magnetic stirrer. The tube was thermostated at T = 313.15 K in a water bath T-3.1 equipped with a precise temperature controller MIT-8.15 "Iztech" (Russia). The actual temperature was recorded with a PTSV-4.2 "Kriotherm" (Russia) thermocouple with an accuracy of 0.02 K. The mass growth during the absorption process was controlled at regular intervals with the Shimadzu AUW220D electronic scales without buoyancy correction. The CO_2-saturated

https://doi.org/10.1021/acs.jced.2c00245
J. Chem. Eng. Data 2022, 67, 2899−2912

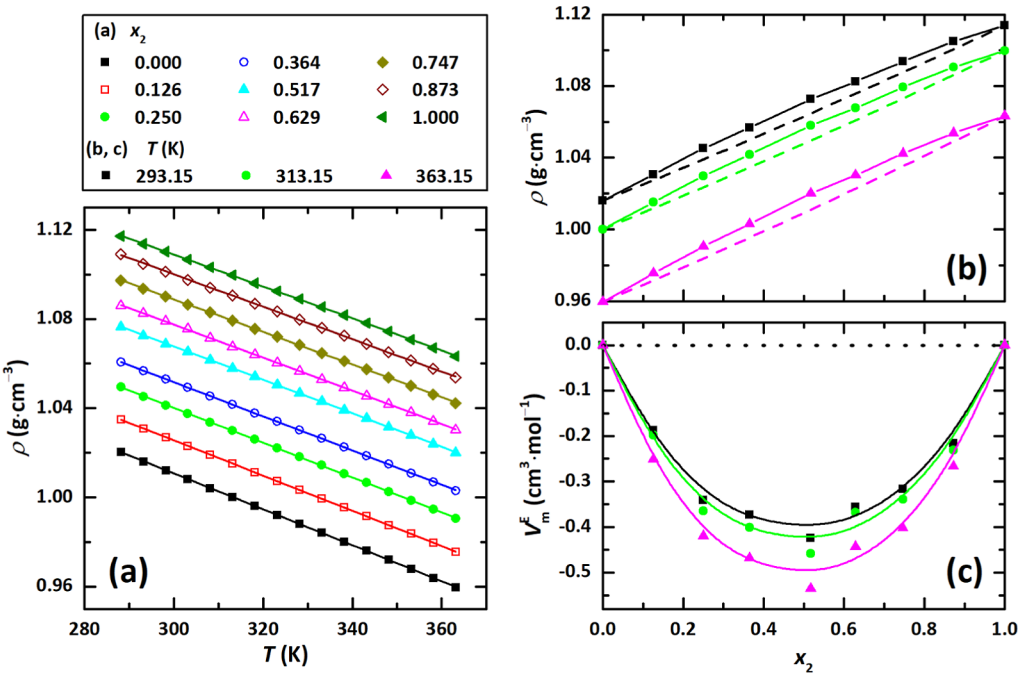

Figure 1. Densities (ρ) (a,b) and excess molar volumes (V_m^E) (c) of {MEA(1) + EG(2)} mixtures as a function of (a) temperature (T) and (b,c) EG mole fraction (x_2). Solid lines in (a) are fits with eq 2, a guide for the eye in (b), and fits with the Redlich-Kister equation in (c); dashed lines in (b) show ideal density at corresponding temperatures; and dotted lines in (c) indicate zero.

samples obtained as such were further used for density and viscosity measurements (see below). A weight loss caused by solvent evaporation was measured by performing blank experiments on bubbling dry nitrogen through a sample and recording the mass loss under the conditions of the CO_2 absorption measurements. Reproducibility of the measurements was found to be within 0.5%. However, taking into account the errors associated with weighing, temperature, and accuracy of mixture preparation, the expanded related uncertainty of the CO_2 capacity expressed on a molality scale (m_{CO_2}) and for MEA efficiency defined as moles of CO_2 absorbed by 1 mole of MEA (c_{CO_2}) was found to be $U_r(m_{CO_2})$= 0.05 and $U_r(c_{CO_2})$= 0.05. As an example, Figure S2 displays the CO_2 absorption profiles for the {MEA(1) + EG(2) + ChCl(3)} system, exhibiting a constant MEA/EG mole ratio of x_1/x_2 = 0.339 and ChCl mole fraction (x_3) varying from 0.005 to 0.215.

The gas absorption measurements were validated at P = 0.1 MPa with 15 and 30 wt % MEA solutions absorbing CO_2 at 298.15 and 313.15 K and DES composed of NH_4SCN and glycerol in a molar ratio 2:3 absorbing NH_3 at 313.15 K. The reference values of their absorption capacity were taken from refs 47−52. As seen in Table S2, the results obtained in the present work are in good agreement with the data obtained by Huertas *et al.*[47] Deng *et al.*[48] and Li *et al.*[49] also found by the gravimetric method and in reasonable accordance with the volumetric measurements by Lee *et al.*[50] Jou *et al.*[51] and Shen co-workers.[52]

RESULTS AND DISCUSSION

Density. To begin with, the properties of the binary mixtures of MEA (1) and EG (2) were investigated. The $\rho(T)$ data of the {MEA + EG} mixtures are summarized in Table 2; Figure 1a displays the $\rho(T)$ data (symbols) together with their linear correlations (lines)

$$\rho = a_0 + a_1 T \tag{3}$$

with a_0 and a_1 fitting coefficients together with their standard deviations being collected in Table S3. The quality of the obtained experimental data was analyzed in terms of their deviations (δ) from the fit with eq 2. According to this analysis, for all of the studied {MEA + EG} mixtures, the maximum deviations lie within the $-0.04 \le 100\delta \le +0.04$ range and thus below the claimed standard uncertainty of $U_r(\rho) \approx 0.001$.

The literature provides a few papers containing density data for the {MEA + EG} system. Yang *et al.*[53] investigated the mixtures covering an entire miscibility range within the temperature range of T = (283.15 to 343.15) K; Tsierkezos and Molinou[54] studied densities at 293.15 K, and Jae-Hoon Song and co-workers[55] performed measurements for {MEA + EG} solutions with w_{MEA} = 15.3% (x_2 = 0.8449) and w_{MEA} = 30.0% (x_2 = 0.6966) at temperatures from 303.15 to 343.15 K. Figure S3 compares the present data with the literature in the spirit of a deviation of experimental data from the fit (δ) according to eq 2 as a function of x_2 at T = 293.15 K (a) and as a function of T (b); the coefficients for the $\rho = f(x_2)$ polynomial fits at temperatures of interest are listed in Table S4.

As seen in Figure S3a, the present data deviate around the $\rho = f(x_2)$ fit within the estimated uncertainty ($|100\delta| < 0.1$). As for the data in ref 53, the deviations are within the mentioned limit for $x_2 < 0.4$ and x_2 = 0.8999. For other compositions, 100δ exceeds the ±0.1 limit and reaches −0.16 for neat EG. Even greater negative deviations are observed for the data by Tsierkezos and Molinou.[54] Here, $|100\delta|$ is within the uncertainty interval only for the mixtures with $x_2 < 0.3$ and pure EG, but for the mixtures with $0.2907 \le x_2 \le 0.9527$, $|100\delta|$ is always greater than 0.1 with a maximum of 0.42 for a

https://doi.org/10.1021/acs.jced.2c00245
J. Chem. Eng. Data 2022, 67, 2899−2912

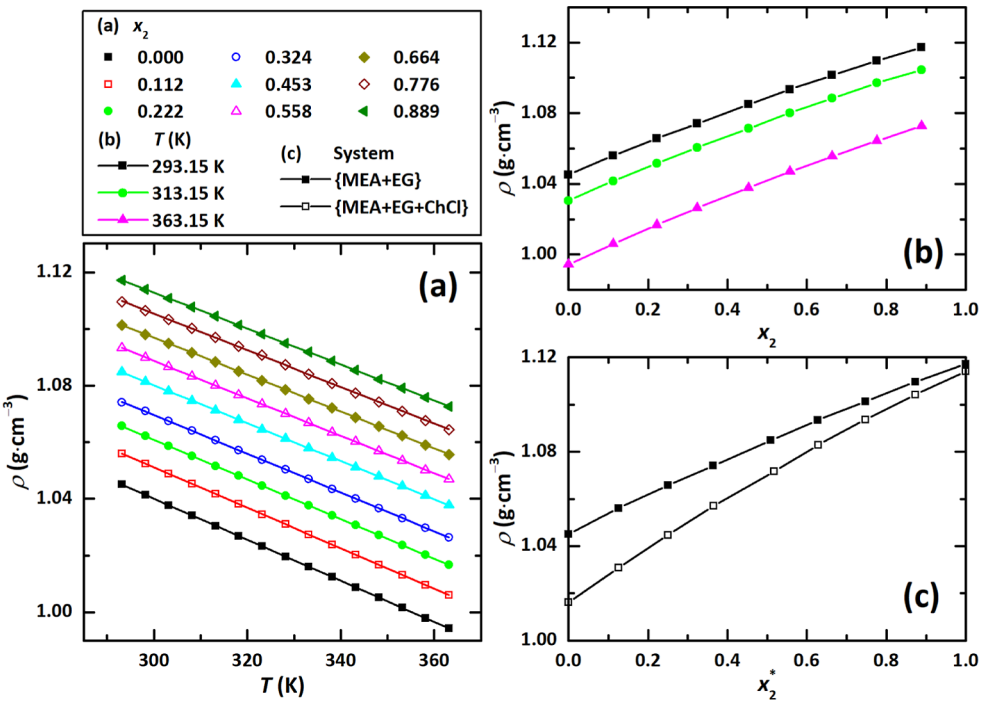

Figure 2. Densities (ρ) (a,b) of {MEA(1) + EG(2) + ChCl(3)} mixtures and a comparison with the binary {MEA + EG} mixture at T = 293.15 K (c) as a function of (a) temperature (T), (b) EG mole fraction (x_2), and (c) EG mole fraction (x_2^*, see text). Solid lines in (a) are fits with eq 2 and a guide for the eye in (b,c).

solution with x_2 = 0.7010. Also, the data in ref 55 (Figure S3b) are systematically lower than those of the present fit by approximately 0.15 for a solution with w_{MEA} = 15.3% and by approximately 0.2 for w_{MEA} = 30.0%. Since in all of the mentioned studies, the mass fraction purity of individual mixture components was comparable to that of our study, the purity of the samples can be ruled out as a reason the observed differences. This conclusion is supported by rather good agreement of the density data obtained for pure MEA and EG. In principle, an increased water content (compared to that of the reference samples) can decrease DES density within the observed limits. However, since none of the mentioned papers provide the remaining water content for their mixtures and the expanded relative uncertainties for their measurements, it is not possible to reveal the real reasons for the differences observed for the discussed experimental data.

As expected from the neat solvents' density (Table 2), an increase in EG content promotes a gradual increase in ρ (Figure 1a) with an obvious positive deviation from ideality (Figure 1b). In order to estimate the origin of the system non-ideality, Figure 1c displays excess molar volumes (V_m^E) estimated as following

$$V_m^E = \frac{(x_1M_1 + x_2M_2)}{\rho} - \left(\frac{x_1M_1}{\rho_1} + \frac{x_2M_2}{\rho_2}\right) \quad (4)$$

with ρ, ρ_1, and ρ_2 representing densities of the mixture, pure MEA (1), and EG (2), respectively, and other parameters being defined above.

As seen in Figure 1c, for the studied {MEA + EG} system, V_m^E values are negative over an entire composition and temperature range. Negative V_m^E values are indicative of a compression of the system volume, which may be caused by strong attractive interactions (*e.g.*, H bonding), and packing of the molecules in the cavities formed when an inherent structure of the solvent breaks down or both of the mentioned effects. In principle, V_m^E is the property showing an overall effect, but the analysis of its temperature dependence can reveal which one dominates in the studied system. Thus, positive $\partial V_m^E/\partial T$ values indicate predominance of the H bonding effects as H bonds are extremely sensitive to temperature. Negative $\partial V_m^E/\partial T$ values point out that with an increase in T, the structure of the mixture becomes more compact compared to that of an ideal solution, which means that packing effects play a more significant role. The fact that, in the {MEA + EG} mixture, V_m^E increases with increasing T clearly indicates that packing effects rather than H bonding govern the system density. However, as expected from substances comprising the system and as it will be shown from the analysis of viscosity (see below), H-bonding still plays an important role as the excess viscosity is positive and shows a negative correlation with temperature.

An effect of ChCl on volumetric properties of neat and mixed solvents was estimated by analyzing their density in the presence of the salt in a constant amount of x_3 = 0.111 but various MEA/EG ratios. The experimentally obtained ρ data for all of the studied {MEA + EG + ChCl} mixtures are summarized in Table 3, and Figure 2 displays the ρ data as a function of T (a) and EG mole fraction (b) and (c) demonstrates the property with (full symbols) and without (open symbols) ChCl at T = 293.15 K. Note, that in order to simplify the perception of these comparison, EG mole fraction was expressed as

$$x_2^* = n_1/(n_1 + n_2) \quad (5)$$

that is, $x_2^* = x_2$ for binary {MEA + EG} and $x_2^* = x_2 + 0.111$ for ternary {MEA + EG + ChCl} mixtures.

For the studied ternary mixtures, the deviations of the experimental data from the fit with eq 2 never exceeded the

https://doi.org/10.1021/acs.jced.2c00245
J. Chem. Eng. Data 2022, 67, 2899−2912

$-0.03 \leq 100\delta \leq +0.02$ interval, which is significantly below the estimated expanded uncertainty of $U_r(\rho) = 0.001$. This indicates a good quality of the obtained data and assures that the observed effects can be definitely assigned to the presence of ChCl. Figure S4a compares density data for the {MEA + ChCl} solution ($x_3 = 0.111$) with those by Mjalli *et al.*,[56] obtained within the temperature range of $T = (298.15$ to $358.15)$ K. As clearly seen, the latter are significantly higher with deviations being at the level of 2%. Since the chemicals used by the authors were of comparable purity, such difference cannot be explained by the presence of impurities. In addition, although the expanded uncertainties for the measurements and water content for the samples were not provided by the authors, it is very unlikely that these factors can influence the data to such an extent. Much better agreement between the present data with the data obtained in the literature for {MEA + EG + ChCl} mixtures with other compositions hints at problems with quality of the data in Ref 56.

As seen in Figure 2b,c, addition of ChCl to the {MEA + EG} mixed solvents does not influence the trend observed for the binary {MEA + EG} mixtures, that is, density increases with an increase in the EG content. The effect, however, is getting more pronounced for the mixtures containing greater amount of MEA (see Figure 2c). For example, in the presence of ChCl, density changes from 1.016 to 1.045 g·cm^{-3} and from 1.114 to 1.117 g·cm^{-3} for MEA ($x_2 = 0.000$) and EG ($x_1 = 0.000$) solutions, respectively. This observation can be explained by different values of ChCl apparent molar volume (V_3^φ) in the mixed {MEA + EG} solvents. For constant ChCl, mole fraction (x_3) can be estimated as

$$V_3^\varphi = \frac{M_3}{\rho} - \left[\frac{(\rho - \rho_0)(1 - x_3)}{\rho\rho_0 x_3}\right] \quad (6)$$

where M_3 is ChCl molar mass and ρ and ρ_0 represent density of the ternary {MEA + EG + ChCl} and binary {MEA + EG} mixtures, respectively. The V_3^φ values plotted as a function of x_2 are shown in Figure S5. They gradually increase with increasing EG content from $V_3^\varphi = 120.2$ cm^3 mol^{-1} at $x_2 = 0.000$ to $V_3^\varphi \approx 123.7$ cm^3 mol^{-1} at $x_2 = 0.6$ and remain rather constant at higher EG concentrations.

In order to estimate an effect of ChCl in an amount of $x_3 = 0.111$ on the structure of {MEA + EG}, Hepler's constant $\left(\frac{\partial^2 V_3^\varphi}{\partial T^2}\right)_p$ was estimated for all of the studied mixed solvent compositions.[57,58] To do this, temperature dependencies of V_3^φ were fitted with the following equation[59]

$$V_3^\varphi = A + BT + CT^2 \quad (7)$$

where A, B, and C are the fitting parameters. Temperature dependencies of V_3^φ together with their fits with eq 7 are plotted in Figure S6.

Positive values of Hepler's constant—which can be calculated as $\left(\frac{\partial^2 V_3^\varphi}{\partial T^2}\right)_p = 2C$—indicate the existence of structure-making effects of a solute, while negative values are associated with its structure-breaking character. As seen in Table S5, the $\left(\frac{\partial^2 V_3^\varphi}{\partial T^2}\right)_p$ values are negative for all compositions of the mixed solvent but constant ChCl content. Hence, it can be argued that ChCl in an amount of $x_3 = 0.111$ acts as a structure breaker with respect to the mixed {MEA + EG} solvent over its entire composition range.

In order to estimate how an increase in ChCl concentration influences properties of the {MEA + EG + ChCl} mixtures, density of the solutions with ChCl mole fraction (x_3) varying from 0.005 to 0.215 but a fixed MEA to EG mole ratio of $x_1/x_2 = 0.339$ was also investigated. This composition was chosen in accordance with the CO_2 absorption experiments, which revealed the smallest mass loss for the {MEA + EG} mixture exhibiting this molar ratio.

Densities of this system within the temperature range $T = (288.15$ to $363.15)$ K are collected in Table 4 and Figure 3

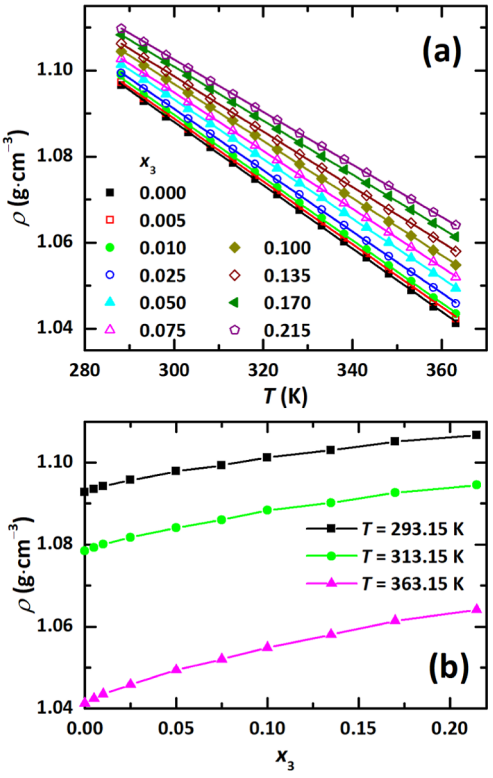

Figure 3. Densities (ρ) of {MEA(1) + EG(2) + ChCl(3)} mixtures with a constant x_1/x_2 molar ratio of 0.339 as a function of (a) temperature (T) and (b) ChCl mole fraction (x_3). Solid lines in (a) are fits with eq 2 and a guide for the eye in (b).

shows the ρ dependencies on temperature (a) and EG mole fraction (b) with symbols corresponding to the experimentally obtained data. These deviate around the fit (Figure 4a, lines) with eq 3 within the interval not exceeding the 100δ values from -0.04 for the lower and $+0.02$ for the upper limits; coefficients a_0 and a_1 of these linear correlations are listed in Table S3. As seen in Figure 3a,b, an increase in ChCl concentration leads to a gradual increase in the solution density.

Although not for all solutions, it was possible to measure density of the CO_2-loaded samples, the trends shown in Figure S7a–c indicate that density is higher for the samples containing greater amount of MEA. This is the case for both binary and ternary mixtures containing constant amount of ChCl. For the system comprising a fixed MEA/EG molar ratio, this trend tends to be same as with a x_3 increase, density of the CO_2-loaded samples decreases. Obviously, this is in agreement

https://doi.org/10.1021/acs.jced.2c00245
J. Chem. Eng. Data 2022, 67, 2899–2912

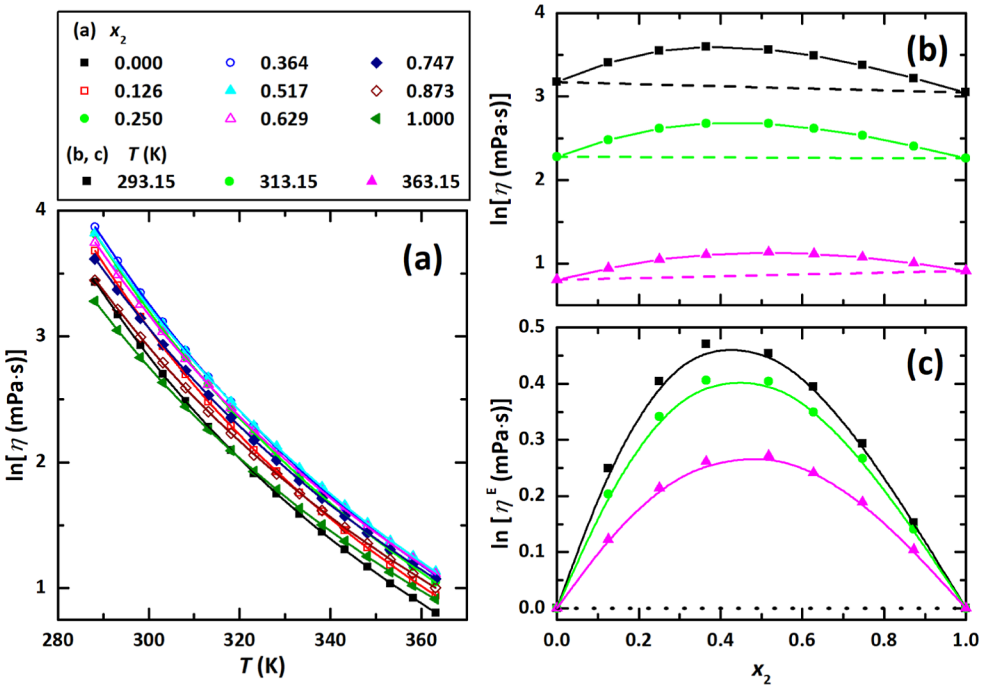

Figure 4. Logarithmic viscosities ($\ln\eta$) (a,b) and excess logarithmic viscosities ($\ln\eta^E$) (c) of {MEA(1) + EG(2)} mixtures as a function of (a) temperature (T) and (b,c) EG mole fraction (x_2). Solid lines in (a) are fits with eq 2, a guide for the eye in (b), and the fits with the Redlich−Kister equation in (c); dashed lines in (b) show ideal logarithmic viscosity at corresponding temperatures; and dotted lines in (c) indicate zero.

with the above statement as when x_3 increases from 0.000 to 0.215, x_1 decreases from 0.252 to 0.210.

Viscosity. Viscosities (η) of the binary {MEA + EG} and ternary {MEA + EG + ChCl} mixtures with x_3 = 0.111 and a constant x_1/x_2 molar ratio of 0.339 are collected in Tables 5−7, respectively. The empirical Vogel−Fulcher−Tammann (VFT) equation

$$\ln\frac{\eta}{\eta_0} = \ln\left(\frac{A_\eta}{\eta_0}\right) + \frac{B_\eta}{T - T_{0,\eta}} \tag{8}$$

was used to fit the experimental data (η) as a function of temperature (T). In eq 8, η_0 = 1 mPa•s, A_η is a viscosity limit at $T \to \infty$, B_η is a parameter linked to a pseudoactivation energy, and $T_{0,\eta}$ is the so-called VFT temperature. Parameters of eq 8 are given in Table S6. For all of the experimental points, a deviation from the fit does not exceed the limits of 100δ from −0.68 to +0.71, which are lower than the estimated relative expanded uncertainty of $U_r(\eta)$ = 0.02. Plotted as a function of x_2 (see Figure S8 and Table S7 for the corresponding fitting parameters), the viscosity data deviate within the $-0.33 \le 100\delta \le +0.37$ interval (T = 293.15 K) and, thus, similar to the $\eta(T)$ dependencies, within the limits of estimated uncertainties. The data by Tsierkezos and Molinou[54] (Figure S8a) show good agreement with the present fit only for mixtures with $x_2 < 0.5$ and pure EG. For $0.4960 \le x_2 \le 0.9527$, the data are much lower with a maximum of $100\delta = -10.5$ at x_2 = 0.8691. Even though the density data by Song *et al.*[55] are in a very satisfactory agreement with ours, their viscosities agree very well (Figure S8b) with the present fit within a whole temperature range for both the studied mixture compositions. However, we here recall again that due to the reasons given above, it is difficult to discuss the real reasons of difference between the present data and viscosities given in refs54 and.[55]

Figure 4 shows the experimental ln η data as a function of T (a) and EG mole fraction (b) together with the result of a fit (lines, a) and a property (ln η^{id}) expected from an ideal mixing (dashed lines, b); Figure 4c displays an excess logarithmic viscosity (ln η^E) defined here as

$$\ln\eta^E = \ln\eta - (x_1\ln\eta_1 + x_2\ln\eta_2) \tag{9}$$

with η being viscosity of the studied binary mixtures and η_1, η_2, x_1, and x_2 representing the viscosity and mole fraction of MEA (1) and EG (2), respectively. The second term corresponds to ideal viscosity ($\ln\eta^{id} = x_1 \ln\eta_1 + x_2 \ln\eta_2$), whose efficiency was approved by Kendall and Monroe.[60]

As seen in Figure 4b and Table 5, viscosity of the binary {MEA + EG} mixture passes through a maximum at $x_2 \approx 0.4$ at 293.15 K and $x_2 \approx 0.5$ at 293.15 K. The presence of a maximum indicates significant deviations from viscosity of an ideal mixture exhibiting no interactions between system components (dashed lines in Figure 4b). Non-ideality of the {MEA + EG} mixtures become less pronounced with an increase in T, which is reflected in the negative values of $\partial\ln\eta^E/\partial T$. In general, such a behavior suggests that the number and/or the intensity of the H bonds formed between mixture components, MEA and EG, is greater/weaker than that between molecules in neat solvents, that is, MEA−MEA and EG−EG interactions. As a result, the overall dynamics of the mixed solvent slows down, leading to a significant increase in its viscosity. Although, this conclusion is in full agreement with the conclusions drawn from the analysis of V^E, see Figure 1c, a direct analysis of the strength and number of the H bonds formed between the system components is only possible by engaging spectroscopic analysis and/or molecular dynamics simulations.

When fixed amount of ChCl (x_3 = 0.111) is added to a mixed {MEA + EG} solvent, its viscosity increases with a

https://doi.org/10.1021/acs.jced.2c00245
J. Chem. Eng. Data 2022, 67, 2899−2912

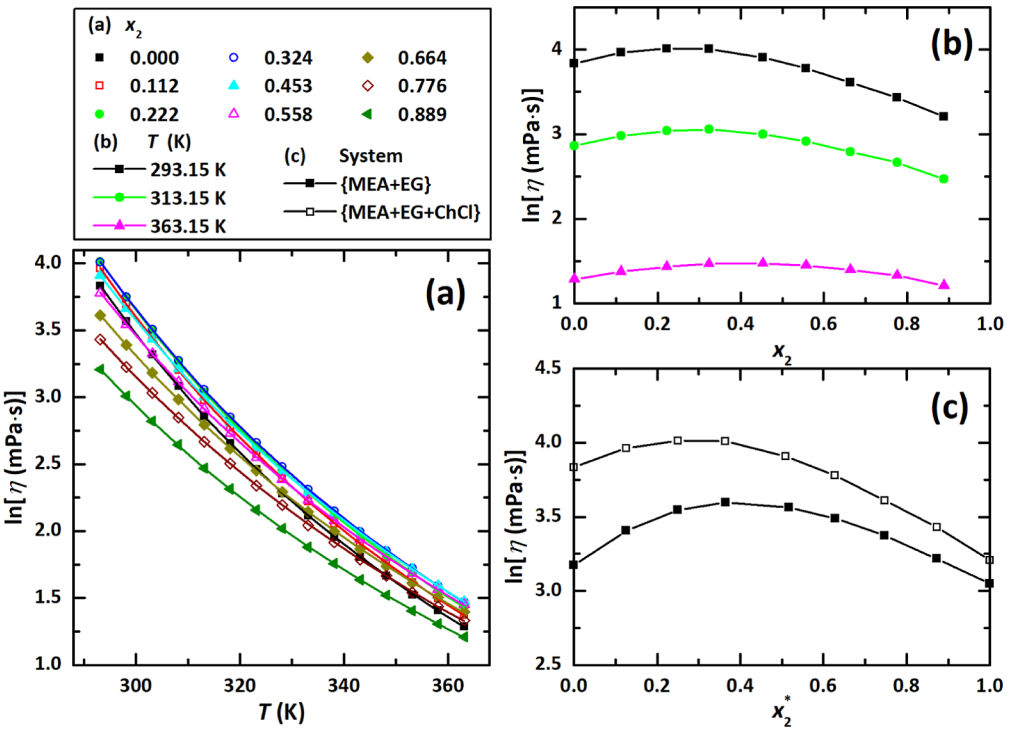

Figure 5. Logarithmic viscosities ($\ln\eta$) of {MEA(1) + EG(2) + ChCl(3)} mixtures (a,b) and a comparison with the binary {MEA + EG} mixture at T = 293.15 K (c) as a function of (a) temperature (T), (b) EG mole fraction (x_2), and (x_2^*, see text). Solid lines in (a) are fits with eq 7 and a guide for the eye in (b,c).

ChCl-related contribution gradually decreasing with increasing x_2, see Figure 5c. A greater influence of ChCl on $\ln\eta$ in the case of MEA solutions indicates stronger charge−charge and/or solute−solvent interactions compared to those in ChCl solutions in EG. However, more information on the type of interactions and their predominance in the studied system can be only extracted from diluted-region concentration dependencies of viscosity, for example, by the analysis of the coefficients of the Jones−Dole equation.

The data for the {MEA + ChCl} solution with x_3 = 0.111 were compared to those in ref 56, see Figure S4b. The latter deviate around the fit within the $-9.7 \leq 100\delta \leq 5.8$ interval. The parabolic trend of the observed deviation is obviously due to different fitting equations: although Mjalli *et al.*[56] used the Arrhenius equation to describe their experimental data, the VFT dependence worked better for the present viscosity data.

It is interesting to note that in the presence of ChCl, an overall trend of viscosity for the systems with various MEA/EG molar ratios does not change compared to that of the mixed {MEA + EG} solvent. Moreover, ChCl has almost no influence on the position of the viscosity maximum and its temperature-induced trend, see Figures 4b and 5b. Apparently, even high ChCl concentrations do not really affect the number and intensity of H bonds formed between the molecular solvent components. However, since no direct H-bond analysis has been performed, the above suggestions can only be taken with a grain of salt.

Similar to density experiments, the effect of ChCl concentration was investigated with the mixture comprising a constant x_1/x_2 molar ratio of 0.339. Figure 6 displays temperature (a) and concentration (b) dependencies of the property. As seen, with an increase in ChCl concentration, viscosity gradually increases from 23.3 for neat solvent to 40.8 mPa•s for the solution with x_3 = 0.215 at 298.15 K.

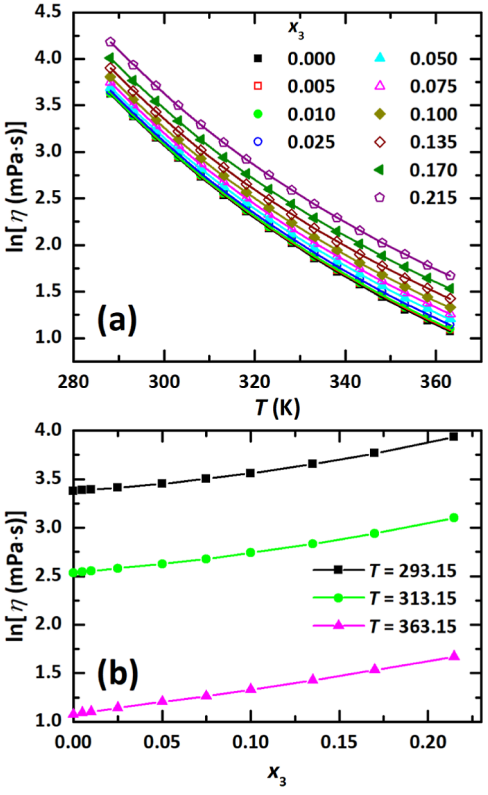

Figure 6. Viscosities (η) of {MEA(1) + EG(2) + ChCl(3)} mixtures at a constant x_1/x_2 molar ratio of 0.339 as a function of (a) temperature (T) and (b) ChCl mole fraction (x_3). Solid lines in (a) are fits with eq 7 and a guide for the eye in (b).

https://doi.org/10.1021/acs.jced.2c00245
J. Chem. Eng. Data 2022, 67, 2899−2912

Comparison of viscosity for the neat and CO_2-loaded samples at T = 298.15 K is shown in Figure S7d–f. Similar to density, η of the CO_2-loaded samples is always greater than that for neat samples and increases with increasing MEA concentration, regardless of whether binary or ternary mixtures are considered.

CO_2 Absorption Capacity. CO_2 absorption capacity of the systems comprising a constant ChCl amount of x_3 = 0.111 (a) and a fixed x_1/x_2 molar ratio of 0.339 (b) obtained gravimetrically is shown in Figure 7 and collected in Table S8. As clearly seen in Figure 7a, with increasing MEA fraction (x_1), an increase in the CO_2 absorption capacity (m_{CO_2}) is observed. This is quite common as the present mixtures (except for those with x_1 = 0.000) exhibit chemical CO_2 capture. Such a trend has been already observed also for DES-related systems, for example, an improvement in the CO_2 absorption capacity was found for reline when MEA content increased.[61] Obviously, the lowest CO_2 capacity is observed for the mixtures not containing MEA, for example, for the one consisting of ChCl (x_3 = 0.111) and EG (x_2 = 0.889), as only physical absorption can be implemented by these systems. Absorbing capacity of this solution (m_{CO_2} = 0.0536 $mol_{CO_2}/kg_{solution}$) is higher than that for ethaline (m_{CO_2}) = 0.0239,[62] 0.0222,[56] and 0.0131[63] $mol_{CO_2}/kg_{solution}$, a mixture of ChCl and EG in a mole ratio of 1:2, found by interpolation of the m_{CO_2} versus P[56,62] and P versus x_{CO_2}[63] data obtained under the same experimental conditions with the volumetric method. Although we agree that more data are necessary for finding a correlation, this comparison suggests negative effects of ChCl on the absorption capacity of EG.

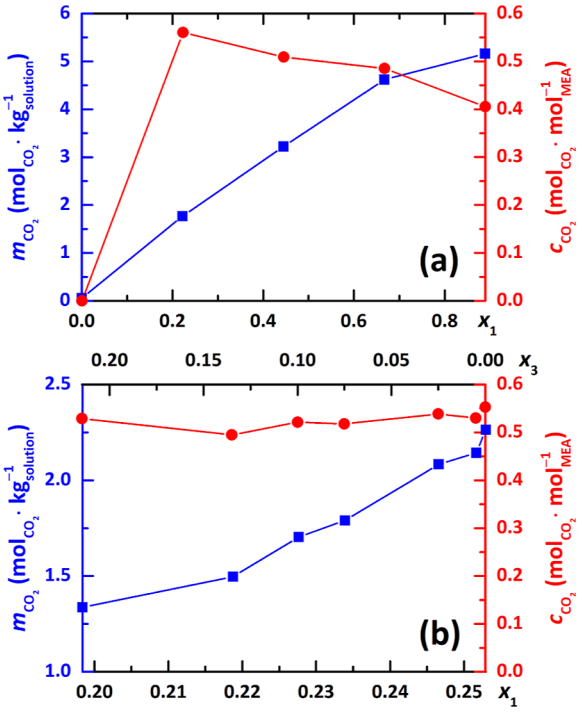

Figure 7. CO_2 absorption capacity (m_{CO_2}, blue) and MEA efficiency (c_{CO_2}, red) of the ternary {MEA(1) + EG(2) + ChCl(3)} mixtures containing a constant mole fraction of ChCl (x_3 = 0.111), (a) and a fixed x_1/x_2 molar ratio of 0.339 (b) as a function of MEA (x_1) and ChCl (x_3) mole fractions at T = 313.15 K.

For the absorbing mixtures with a constant molar fraction of ChCl (x_3 = 0.111) and x_1 > 0.000, the CO_2 efficiency decreases from c_{CO_2} = 0.560 for x_1 = 0.225 to 0.406 mol_{CO_2}/mol_{MEA} for x_1 = 0.777. However, their absorption capacity expressed on a molality scale is rather proportional to MEA content and, for the mentioned systems, increases from m_{CO_2} = 1.77 to 5.16 $mol_{CO_2}/kg_{solution}$. Thus, similar to other aqueous[61] and also non-aqueous[27] absorbing mixtures, the efficiency of MEA in the present solutions depends on its content and is higher for diluted solutions.

A further analysis was aimed at investigation of the effect of ChCl concentration on the system absorption capacity and MEA efficiency. The choice of the system was based on the following issues. First, we looked for a mixed solvent with a MEA/EG ratio exhibiting both high MEA efficiency and good absorption capacity. Second, the mixture should be as non-volatile as possible. Blank experiments with purging nitrogen showed that under experimental conditions used in this work, a mixture with ChCl/EG/MEA = 1:6:2 shows the smallest mass loss compared to that of other studied solutions. In addition, this mixture possesses good CO_2 absorption capacity of m_{CO_2} = 1.77 $mol_{CO_2}/kg_{solution}$ and an efficiency of c_{CO_2} = 0.560 mol_{CO_2}/mol_{MEA}. As a result, this mixed solvent with a MEA to EG mole ratio of x_1/x_2 = 0.339 was chosen for further investigation.

As seen in Figure 7b, c_{CO_2} does not change significantly when ChCl content increases from x_3 = 0.000 to 0.215. However, as far as CO_2 capacity is considered, again, m_{CO_2} steadily increases with increasing MEA content. This means that, in principle, addition of a significant amount of ChCl cannot improve the overall capacity of the {MEA + EG} mixtures. However, taking into account attractiveness of DES-associated systems as technological solvents,[64] these findings are of interest for developing new absorbing systems.

CONCLUSIONS

Due to an increasing scientific interest in using DESs and related systems as efficient CO_2-absorbing media in the present paper, we systematically analyze the influence of salt and amine concentration on the absorption properties of mixtures composed of MEA, EG, and ChCl. We show that absorption capacity of the mixtures expressed in moles of CO_2 dissolved in 1 kg of a solution always increases with an increase in MEA concentration. A character of this increase clearly points at the chemical nature of the CO_2 absorption by the studied system implemented using MEA molecules. This suggestion is supported by the fact that the picture is opposite when MEA absorption efficiency is considered. Here, the number of moles of CO_2 absorbed by 1 mole of MEA decreases when MEA concentration increases. Interestingly, both the above observations are true for the ternary mixtures, regardless of the presence of ChCl. In principle, its addition to the mixed solvent decreases CO_2 absorption capacity of the {MEA + EG} system. However, the observed trend is rather caused by a decrease in the overall MEA concentration as MEA efficiency is not affected by the presence of ChCl. As far as EG is considered as a mixture component, it serves a MEA co-solvent exhibiting in addition rather high CO_2 physisorption. Unfortunately, comparison of the present data for a binary {EG + ChCl} mixture with the data provided in the literature

https://doi.org/10.1021/acs.jced.2c00245
J. Chem. Eng. Data 2022, 67, 2899–2912

does not allow one to find clear correlations between the ChCl/EG mole ratio and its ability to absorb CO_2.

In addition, such industrially important physical properties as density (ρ) and viscosity (η) of the binary {MEA + EG} and ternary {MEA + EG + ChCl} mixtures were investigated within a wide range of temperatures for both neat and CO_2-loaded samples. When MEA is added to neat EG, both properties show positive deviations from the trends expected for an ideal mixing. Analysis of the excess properties and their temperature dependencies reveals that for density, these deviations are mainly caused by packing effects. However, H bonding still significantly contributes to density and plays a leading role when changes in viscosity are considered. Addition of a fixed amount of ChCl to the mixed {MEA + EG} solvent increases its density and viscosity over an entire range of mixture composition with the contribution decreasing with an increase in EG content. Similarly, both ρ and η show a steady increase when ChCl is added to {MEA + EG} with a fixed MEA/EG molar ratio. In general, one can conclude that ChCl acts as a structure breaker with respect to the mixed {MEA + EG} solvent. For the CO_2-loaded samples, both ρ and η are significantly higher compared to those of neat samples with the contribution being greater for the mixtures with higher MEA content.

■ ASSOCIATED CONTENT

Supporting Information

The Supporting Information is available free of charge at https://pubs.acs.org/doi/10.1021/acs.jced.2c00245.

Additional experimental data, including validation experiments, remaining water content, CO_2 absorption capacity (m_{CO_2}) as a function of time (t), absorption capacity (m_{CO_2}), and amine efficiency (c_{CO_2}); calculated coefficients obtained by fitting the experimental data with the equations, Helper's constants; and comparison of the obtained data with the literature (PDF)

■ AUTHOR INFORMATION

Corresponding Author

Olga V. Kazarina − *Nizhny Novgorod State Technical University n.a. R.E. Alekseev, Nizhny Novgorod 603950, Russian Federation; Mendeleev University of Chemical Technology, Moscow 125047, Russian Federation;* orcid.org/0000-0002-4841-2739; Email: olga_kazarina@list.ru

Authors

Vira N. Agieienko − *Nizhny Novgorod State Technical University n.a. R.E. Alekseev, Nizhny Novgorod 603950, Russian Federation;* orcid.org/0000-0002-9398-1666

Anton N. Petukhov − *Mendeleev University of Chemical Technology, Moscow 125047, Russian Federation; Lobachevsky State University of Nizhny Novgorod, Chemical Engineering Laboratory, Research Institute for Chemistry, Nizhny Novgorod 603950, Russian Federation;* orcid.org/0000-0002-4904-7622

Andrey V. Vorotyntsev − *Nizhny Novgorod State Technical University n.a. R.E. Alekseev, Nizhny Novgorod 603950, Russian Federation; Lobachevsky State University of Nizhny Novgorod, Chemical Engineering Laboratory, Research Institute for Chemistry, Nizhny Novgorod 603950, Russian Federation;* orcid.org/0000-0001-5447-5296

Alexander S. Kazarin − *Lobachevsky State University of Nizhny Novgorod, Chemical Engineering Laboratory, Research Institute for Chemistry, Nizhny Novgorod 603950, Russian Federation*

Maria E. Atlaskina − *Nizhny Novgorod State Technical University n.a. R.E. Alekseev, Nizhny Novgorod 603950, Russian Federation; Mendeleev University of Chemical Technology, Moscow 125047, Russian Federation*

Artem A. Atlaskin − *Mendeleev University of Chemical Technology, Moscow 125047, Russian Federation*

Artyom N. Markov − *Lobachevsky State University of Nizhny Novgorod, Chemical Engineering Laboratory, Research Institute for Chemistry, Nizhny Novgorod 603950, Russian Federation*

Anna A. Golovacheva − *Mendeleev University of Chemical Technology, Moscow 125047, Russian Federation*

Ilya V. Vorotyntsev − *Mendeleev University of Chemical Technology, Moscow 125047, Russian Federation;* orcid.org/0000-0003-2282-0811

Complete contact information is available at: https://pubs.acs.org/10.1021/acs.jced.2c00245

Author Contributions

O.V.K.: writing—original draft, validation, project administration, and funding acquisition. V.N.A.: writing—original draft, visualization, validation, and conceptualization. A.N.P.: methodology. A.V.V.: writing—review and editing. A.S.K.: investigation and writing—review and editing. M.E.A.: formal analysis. A.A.A.: software. A.N.: formal analysis. A.A.G.: investigation. I.V.V.: supervision.

Notes

The authors declare no competing financial interest.

■ ACKNOWLEDGMENTS

The main part of this work was supported by the Russian Science Foundation, grant number 21-73-00167. The part related to the investigation an effect of ChCl on the structure of {MEA + EG} and the Hepler's constant estimation was financially supported by the Ministry of Science and Higher Education of the Russian Federation, Laboratory of Ionic Materials (LIM), project no FSSM-2021-0014.

■ REFERENCES

(1) Heuberger, C. F.; Staffell, I.; Shah, N.; Mac Dowell, N. Quantifying the Value of CCS for the Future Electricity System. *Energy Environ. Sci.* **2016**, *9*, 2497−2510.

(2) Paluszny, A.; Graham, C. C.; Daniels, K. A.; Tsaparli, V.; Xenias, D.; Salimzadeh, S.; Whitmarsh, L.; Harrington, J. F.; Zimmerman, R. W. Caprock Integrity and Public Perception Studies of Carbon Storage in Depleted Hydrocarbon Reservoirs. *Int. J. Greenh. Gas Control.* **2020**, *98*, 103057.

(3) White, C. M.; Smith, D. H.; Jones, K. L.; Goodman, A. L.; Jikich, S. A.; LaCount, R. B.; DuBose, S. B.; Ozdemir, E.; Morsi, B. I.; Schroeder, K. T. Sequestration of Carbon Dioxide in Coal with Enhanced Coalbed Methane RecoveryA Review. *Energy Fuel.* **2005**, *19*, 659−724.

(4) Bonto, M.; Welch, M. J.; Lüthje, M.; Andersen, S. I.; Veshareh, M. J.; Amour, F.; Afrough, A.; Mokhtari, R.; Hajiabadi, M. R.; Alizadeh, M. R.; Larsen, C. N.; Nick, H. M. Challenges and Enablers for Large-Scale CO_2 Storage in Chalk Formations. *Earth Sci. Rev.* **2021**, *222*, 103826.

(5) Ringrose, P. S.; Furre, A. K.; Gilfillan, S. M. V.; Krevor, S.; Landrø, M.; Leslie, R.; Meckel, T.; Nazarian, B.; Zahid, A. Storage of Carbon Dioxide in Saline Aquifers: Physicochemical Processes, Key

Constraints, and Scale-Up Potential. *Annu. Rev. Chem. Biomol. Eng.* **2021**, *12*, 471−494.
(6) Celia, M. A.; Bachu, S.; Nordbotten, J. M.; Bandilla, K. W. Status of CO_2 Storage in Deep Saline Aquifers with Emphasis on Modeling Approaches and Practical Simulations. *Water Resour. Res.* **2015**, *51*, 6846−6892.
(7) Zheng, J.; Chong, Z. R.; Qureshi, M. F.; Linga, P. Carbon Dioxide Sequestration via Gas Hydrates: A Potential Pathway toward Decarbonization. *Energy Fuels* **2020**, *34*, 10529−10546.
(8) Akhmetshina, A. I.; Petukhov, A. N.; Gumerova, O. R.; Vorotyntsev, A. V.; Nyuchev, A. V.; Vorotyntsev, I. V. Solubility of H_2S and CO_2 in Imidazolium-Based Ionic Liquids with Bis(2-Ethylhexyl) Sulfosuccinate Anion. *J. Chem. Thermodyn.* **2019**, *130*, 173−182.
(9) Trubyanov, M. M.; Shablykin, D. N.; Mokhnachev, N. A.; Sergeeva, M. S.; Vorotyntsev, A. V.; Petukhov, A. N.; Vorotyntsev, V. M. A Hybrid Batch Distillation/Membrane Process for High Purification Part 1: Energy Efficiency and Separation Performance Study for Light Impurities Removal. *Sep. Purif. Technol.* **2020**, *241*, 116678.
(10) Tsiotsias, A. I.; Charisiou, N. D.; Yentekakis, I. V.; Goula, M. A. The Role of Alkali and Alkaline Earth Metals in the CO_2 Methanation Reaction and the Combined Capture and Methanation of CO_2. *Catalysts* **2020**, *10*, 812.
(11) Ye, R. P.; Ding, J.; Gong, W.; Argyle, M. D.; Zhong, Q.; Wang, Y.; Russell, C. K.; Xu, Z.; Russell, A. G.; Li, Q.; Fan, M.; Yao, Y. G. CO_2 Hydrogenation to High-Value Products via Heterogeneous Catalysis. *Nat. Commun.* **2019**, *10*, 5698.
(12) Koytsoumpa, E. I.; Bergins, C.; Kakaras, E. The CO_2 Economy: Review of CO_2 Capture and Reuse Technologies. *J. Supercrit. Fluids* **2018**, *132*, 3−16.
(13) Atlaskin, A. A.; Kryuchkov, S. S.; Yanbikov, N. R.; Smorodin, K. A.; Petukhov, A. N.; Trubyanov, M. M.; Vorotyntsev, V. M.; Vorotyntsev, I. V. Comprehensive Experimental Study of Acid Gases Removal Process by Membrane-Assisted Gas Absorption Using Imidazolium Ionic Liquids Solutions Absorbent. *Sep. Purif. Technol.* **2020**, *239*, 116578.
(14) Vorotyntsev, A. V.; Petukhov, A. N.; Sazanova, T. S.; Pryakhina, V. I.; Nyuchev, A. V.; Otvagina, K. V.; Markov, A. N.; Atlaskina, M. E.; Vorotyntsev, I. V.; Vorotyntsev, V. M. Imidazolium-Based SILLPs as Organocatalysts in Silane Production: Synthesis, Characterization and Catalytic Activity. *J. Catal.* **2019**, *375*, 427−440.
(15) Stauffer, P. H.; Keating, G. N.; Middleton, R. S.; Viswanathan, H. S.; Berchtold, K. A.; Singh, R. P.; Pawar, R. J.; Mancino, A. Greening Coal: Breakthroughs and Challenges in Carbon Capture and Storage. *Environ. Sci. Technol.* **2011**, *45*, 8597−8604.
(16) Abu-Zahra, M. R. M.; Schneiders, L. H. J.; Niederer, J. P. M.; Feron, P. H. M.; Versteeg, G. F. CO_2 Capture from Power Plants: Part I. A Parametric Study of the Technical Performance Based on Monoethanolamine. *Int. J. Greenh. Gas Control.* **2007**, *1*, 37−46.
(17) Luis, P. Use of Monoethanolamine (MEA) for CO_2 Capture in a Global Scenario: Consequences and Alternatives. *Desalination* **2016**, *380*, 93−99.
(18) Cui, D.; Yan, S.; Guo, X.; Chu, F. Advance in Post-Combustion CO_2 Capture with Alkaline Solution: A Brief Review. *Energy Proc.* **2012**, *14*, 1515−1522.
(19) El Hadri, N.; Quang, D. V.; Goetheer, E. L. V.; Abu Zahra, M. R. M. Aqueous Amine Solution Characterization for Post-Combustion CO_2 Capture Process. *Appl. Energy* **2017**, *185*, 1433−1449.
(20) Ko, Y. G.; Shin, S. S.; Choi, U. S. Primary, Secondary, and Tertiary Amines for CO_2 Capture: Designing for Mesoporous CO_2 Adsorbents. *J. Colloid Interface Sci.* **2011**, *361*, 594−602.
(21) Puxty, G.; Rowland, R.; Allport, A.; Yang, Q.; Bown, M.; Burns, R.; Maeder, M.; Attalla, M. Carbon Dioxide Postcombustion Capture: A Novel Screening Study of the Carbon Dioxide Absorption Performance of 76 Amines. *Environ. Sci. Technol.* **2009**, *43*, 6427−6433.
(22) Chowdhury, F. A.; Yamada, H.; Higashii, T.; Goto, K.; Onoda, M. CO_2 Capture by Tertiary Amine Absorbents: A Performance Comparison Study. *Ind. Eng. Chem. Res.* **2013**, *52*, 8323−8331.
(23) Leites, I. L. Thermodynamics of CO_2 Solubility in Mixtures Monoethanolamine with Organic Solvents and Water and Commercial Experience of Energy Saving Gas Purification Technology. *Energy Convers. Manag.* **1998**, *39*, 1665−1674.
(24) Barzagli, F.; Mani, F.; Peruzzini, M. Efficient CO_2 Absorption and Low Temperature Desorption with Non-Aqueous Solvents Based on 2-Amino-2-Methyl-1-Propanol (AMP). *Int. J. Greenh. Gas Control.* **2013**, *16*, 217−223.
(25) Zhang, J.; Misch, R.; Tan, Y.; Agar, D. W. Novel Thermomorphic Biphasic Amine Solvents for CO_2 Absorption and Low-Temperature Extractive Regeneration. *Chem. Eng. Technol.* **2011**, *34*, 1481−1489.
(26) Heldebrant, D. J.; Koech, P. K.; Glezakou, V. A.; Rousseau, R.; Malhotra, D.; Cantu, D. C. Water-Lean Solvents for Post-Combustion CO_2 Capture: Fundamentals, Uncertainties, Opportunities, and Outlook. *Chem. Rev.* **2017**, *117*, 9594−9624.
(27) Bougie, F.; Pokras, D.; Fan, X. Novel Non-Aqueous MEA Solutions for CO_2 Capture. *Int. J. Greenh. Gas Control.* **2019**, *86*, 34−42.
(28) Hwang, K. S.; Park, S. W.; Park, D. W.; Oh, K. J.; Kim, S. S. Absorption of Carbon Dioxide into Diisopropanolamine Solutions of Polar Organic Solvents. *J. Taiwan Inst. Chem. Eng.* **2010**, *41*, 16−21.
(29) Kang, M. K.; Jeon, S. B.; Cho, J. H.; Kim, J. S.; Oh, K. J. Characterization and Comparison of the CO_2 Absorption Performance into Aqueous, Quasi-Aqueous and Non-Aqueous MEA Solutions. *Int. J. Greenh. Gas Control.* **2017**, *63*, 281−288.
(30) Chen, S.; Chen, S.; Fei, X.; Zhang, Y.; Qin, L. Solubility and Characterization of CO_2 in 40 Mass % N -Ethylmonoethanolamine Solutions: Explorations for an Efficient Nonaqueous Solution. *Ind. Eng. Chem. Res.* **2015**, *54*, 7212−7218.
(31) Barbarossa, V.; Barzagli, F.; Mani, F.; Lai, S.; Stoppioni, P.; Vanga, G. Efficient CO_2 Capture by Non-Aqueous 2-Amino-2-Methyl-1-Propanol (AMP) and Low Temperature Solvent Regeneration. *RSC Adv.* **2013**, *3*, 12349−12355.
(32) Bihong, L.; Kexuan, Y.; Xiaobin, Z.; Zuoming, Z.; Guohua, J. 2-Amino-2-Methyl-1-Propanol Based Non-Aqueous Absorbent for Energy-Efficient and Non-Corrosive Carbon Dioxide Capture. *Appl. Energy* **2020**, *264*, 114703.
(33) Barzagli, F.; Lai, S.; Mani, F.; Stoppioni, P. Novel Non-Aqueous Amine Solvents for Biogas Upgrading. *Energy Fuel.* **2014**, *28*, 5252−5258.
(34) Guo, H.; Li, C.; Shi, X.; Li, H.; Shen, S. Nonaqueous Amine-Based Absorbents for Energy Efficient CO_2 Capture. *Appl. Energy* **2019**, *239*, 725−734.
(35) Barzagli, F.; Giorgi, C.; Mani, F.; Peruzzini, M. Reversible Carbon Dioxide Capture by Aqueous and Non-Aqueous Amine-Based Absorbents: A Comparative Analysis Carried out by ^{13}C NMR Spectroscopy. *Appl. Energy* **2018**, *220*, 208−219.
(36) Pelaquim, F. P.; Barbosa Neto, A. M.; Dalmolin, I. A. L.; Costa, M. C. da. Gas Solubility Using Deep Eutectic Solvents: Review and Analysis. *Ind. Eng. Chem. Res.* **2021**, *60*, 8607−8620.
(37) Marcus, Y. Gas Solubilities in Deep Eutectic Solvents. *Monatshefte fur Chemie* **2018**, *149*, 211−217.
(38) Moura, L.; Kollau, L.; Gomes, M. C. *Solubility of Gases in Deep Eutectic Solvents*; Springer: Cham, 2021; Vol. *56*.
(39) Bhawna; Pandey, A.; Pandey, S. Superbase-Added Choline Chloride-Based Deep Eutectic Solvents for CO_2 Capture and Sequestration. *ChemistrySelect* **2017**, *2*, 11422−11430.
(40) Fu, H.; Hou, Y.; Sang, H.; Mu, T.; Lin, X.; Peng, Z.; Li, P.; Liu, J. Carbon Dioxide Capture by New DBU-Based DES: The Relationship between Ionicity and Absorptive Capacity. *AIChE J.* **2021**, *67*, No. e17244.
(41) Jiang, B.; Ma, J.; Yang, N.; Huang, Z.; Zhang, N.; Tantai, X.; Sun, Y.; Zhang, L. Superbase/Acylamido-Based Deep Eutectic Solvents for Multiple-Site Efficient CO_2 Absorption. *Energy Fuel.* **2019**, *33*, 7569−7577.

https://doi.org/10.1021/acs.jced.2c00245
J. Chem. Eng. Data 2022, 67, 2899−2912

(42) Yan, H.; Zhao, L.; Bai, Y.; Li, F.; Dong, H.; Wang, H.; Zhang, X.; Zeng, S. Superbase Ionic Liquid-Based Deep Eutectic Solvents for Improving CO_2 Absorption. *ACS Sustain. Chem. Eng.* **2020**, *8*, 2523−2530.
(43) Adeyemi, I.; Abu-Zahra, M. R. M.; Alnashef, I. Experimental Study of the Solubility of CO_2 in Novel Amine Based Deep Eutectic Solvents. *Energy Proc.* **2017**, *105*, 1394−1400.
(44) Mahi, M.-R.; Mokbel, I.; Négadi, L.; Jose, J. CO_2 Capture Using Deep Eutectic Solvent and Amine (MEA) Solution. *Cut. Edge Carbon Capture Util. Storage* **2017**, 309−316.
(45) Li, Z.; Wang, L.; Li, C.; Cui, Y.; Li, S.; Yang, G.; Shen, Y. Absorption of Carbon Dioxide Using Ethanolamine-Based Deep Eutectic Solvents. *ACS Sustain. Chem. Eng.* **2019**, *7*, 10403−10414.
(46) Chirico, R. D.; Frenkel, M.; Magee, J. W.; Diky, V.; Muzny, C. D.; Kazakov, A. F.; Kroenlein, K.; Abdulagatov, I.; Hardin, G. R.; Acree, W. E.; Brenneke, J. F.; Brown, P. L.; Cummings, P. T.; de Loos, T. W.; Friend, D. G.; Goodwin, A. R. H.; Hansen, L. D.; Haynes, W. M.; Koga, N.; Mandelis, A.; Marsh, K. N.; Mathias, P. M.; McCabe, C.; O'Connell, J. P.; Pádua, A.; Rives, V.; Schick, C.; Trusler, J. P. M.; Vyazovkin, S.; Weir, R. D.; Wu, J. Improvement of Quality in Publication of Experimental Thermophysical Property Data: Challenges, Assessment Tools, Global Implementation, and Online Support. *J. Chem. Eng. Data* **2013**, *58*, 2699−2716.
(47) Huertas, J. I.; Gomez, M. D.; Giraldo, N.; Garzón, J. CO_2 Absorbing Capacity of MEA. *J. Chem.* **2015**, *2015*, 965015.
(48) Deng, D.; Gao, B.; Zhang, C.; Duan, X.; Cui, Y.; Ning, J. Investigation of Protic NH4SCN-Based Deep Eutectic Solvents as Highly Efficient and Reversible NH3 Absorbents. *Chem. Eng. J.* **2019**, *358*, 936−943.
(49) Li, K.; Fang, H.; Duan, X.; Deng, D. Efficient Uptake of NH_3 by Dual Active Sites NH_4SCN-Imidazole Deep Eutectic Solvents with Low Viscosity. *J. Mol. Liq.* **2021**, *339*, 116724.
(50) Lee, J. I.; Otto, F. D.; Mather, A. E. Equilibrium Between Carbon Dioxide and Aqueous Monoethanolamine Solutions. *J. Appl. Chem. Biotechnol.* **1976**, *26*, 541−549.
(51) Jou, F.-Y.; Mather, A. E.; Otto, F. D. The Solubility of CO_2 in a 30 Mass Percent Monoethanolamine Solution. *Can. J. Chem. Eng.* **1995**, *73*, 140−147.
(52) Shen, K. P.; Li, M. H. Solubility of Carbon Dioxide in Aqueous Mixtures of Monoethanolamine with Methyldiethanolamine. *J. Chem. Eng. Data* **1992**, *37*, 96−100.
(53) Yang, F.; Wang, X.; Wang, W.; Liu, Z. Densities and Excess Properties of Primary Amines in Alcoholic Solutions. *J. Chem. Eng. Data* **2013**, *58*, 785−791.
(54) Tsierkezos, N. G.; Molinou, I. E. Densities and Viscosities of Ethylene Glycol Binary Mixtures at 293.15 K. *J. Chem. Eng. Data* **1999**, *44*, 955−958.
(55) Song, J. H.; Park, S. B.; Yoon, J. H.; Lee, H.; Lee, K. H. Densities and Viscosities of Monoethanolamine + Ethylene Glycol + Water. *J. Chem. Eng. Data* **1996**, *41*, 1152−1154.
(56) Mjalli, F. S.; Murshid, G.; Al-Zakwani, S.; Hayyan, A. Monoethanolamine-Based Deep Eutectic Solvents, Their Synthesis and Characterization. *Fluid Phase Equilib.* **2017**, *448*, 30−40.
(57) Shekaari, H.; Armanfar, E. Apparent Molar Volumes and Expansivities of Aqueous Solutions of Ionic Liquids, l-Alkyl-3-Methylimidazolium Alkyl Sulfate at T = (298.15−328.15) K. *Fluid Phase Equilib.* **2011**, *303*, 120−125.
(58) Shekaari, H.; Mousavi, S. S. Volumetric Properties of Ionic Liquid 1,3-Dimethylimidazolium Methyl Sulfate + Molecular Solvents at T = (298.15−328.15) K. *Fluid Phase Equilib.* **2010**, *291*, 201−207.
(59) Zafarani-Moattar, M. T.; Shekaari, H. Apparent Molar Volume and Isentropic Compressibility of Ionic Liquid 1-Butyl-3-Methyl-imidazolium Bromide in Water, Methanol, and Ethanol at T = (298.15 to 318.15) K. *J. Chem. Thermodyn.* **2005**, *37*, 1029−1035.
(60) Kendall, J.; Monroe, K. P. The Viscosity of Liquids.II.The Viscosity-Composition Curve for Ideal Liquid Mixtures. *J. Am. Chem. Soc.* **1917**, *39*, 1787−1802.
(61) Hsu, Y. H.; Leron, R. B.; Li, M. H. Solubility of Carbon Dioxide in Aqueous Mixtures of (Reline + Monoethanolamine) at T = (313.2 to 353.2) K. *J. Chem. Thermodyn.* **2014**, *72*, 94−99.
(62) Leron, R. B.; Li, M. H. Solubility of Carbon Dioxide in a Choline Chloride−Ethylene Glycol Based Deep Eutectic Solvent. *Thermochim. Acta* **2013**, *551*, 14−19.
(63) Harifi-Mood, A. R.; Mohammadpour, F.; Boczkaj, G. Solvent Dependency of Carbon Dioxide Henry's Constant in Aqueous Solutions of Choline Chloride-Ethylene Glycol Based Deep Eutectic Solvent. *J. Mol. Liq.* **2020**, *319*, 114173.
(64) Sarmad, S.; Mikkola, J.-P.; Ji, X. Carbon Dioxide Capture with Ionic Liquids and Deep Eutectic Solvents: A New Generation of Sorbents. *ChemSusChem* **2017**, *10*, 324−352.

Recommended by ACS

Densities, Viscosities of Pure 1-(2-Hydroxyethyl) Pyrrolidine, 3-Amino-1-Propanol, Water, and Their Mixtures at 293.15 to 363.15 K and Atmospheric Pressure
Ardi Hartono and Hanna K. Knuutila
FEBRUARY 23, 2023
JOURNAL OF CHEMICAL & ENGINEERING DATA
READ

Vapor–Liquid Equilibrium Measurements and Cubic-Plus-Association Modeling of Triethylene Glycol + Water + Methane Systems at 6.0 and 12.5 MPa
Julia Trancoso, Nicolas von Solms, *et al.*
DECEMBER 15, 2022
JOURNAL OF CHEMICAL & ENGINEERING DATA
READ

Isobaric Vapor–Liquid Equilibrium for Ethyl Acetate + Chloroform with Ionic Liquids [EMIM][OAc], [BMIM][OAc], and DMSO + [EMIM][OAc] as Entrainers ...
Pengqi Li, Huisheng Feng, *et al.*
JANUARY 04, 2023
JOURNAL OF CHEMICAL & ENGINEERING DATA
READ

Measurements of Isothermal Vapor–Liquid Equilibrium and Critical Point-Based Perturbed-Chain Statistical Association Fluid Theory Phase Behavior Modeling of the Propane +...
Vener F. Khairutdinov, Ilmutdin M. Abdulagatov, *et al.*
DECEMBER 20, 2022
JOURNAL OF CHEMICAL & ENGINEERING DATA
READ

https://doi.org/10.1021/acs.jced.2c00245
J. Chem. Eng. Data 2022, 67, 2899−2912